

DETERMINATION OF CENTROID OF CCD STAR IMAGES

C. Fosu^{a *}, G W. Hein^b, B. Eissfeller^b

^a Dept. of Geodetic Engineering, KNUST, Kumasi Ghana – fosucoll@hotmail.com

^b Institute of Geodesy and Navigation, University FAF Munich Germany –
(guenter.hein, eissfeller)@unibw-muenchen.de

Commission III, WG III/8

KEY WORDS: CCD Star Images, image co-ordinates, astro-geodetic co-ordinates, precise geoids, psf fitting, image moment analysis, centroid estimation, sub-pixel accuracy

ABSTRACT:

The new microchip and sensor technology, *charged couple device (CCD)*, has assumed a permanent position as the natural transducer for optical input to a computer. The CCD combined with the microcomputer have revolutionised the whole discipline of observational astronomy at all stages from data gathering to data analysis, presentation and use. Not only has it brought the convenience of digital imaging to field astronomy but has also great potential in determining very accurate astronomic co-ordinates of a point at great speed and ease, compatible to GPS for the determination of deflection of the vertical and local or precise geoids. Despite the numerous advantages of the CCD in astronomical work most CCD users agree that individual devices have imperfections or various problems that have to be dealt with. In using CCD in geodetic astronomy one major problem that has to be considered is whether the measuring accuracy of the image co-ordinates will be enough for the determination of astronomic latitude or longitude. Just clicking on a star object in a digital image to determine its position in the image yields pixel accuracy. But to meet geodetic accuracies, sub-pixel accuracies are required. In this work we employed least squares smoothing techniques on data obtained from astronomical observations using CCD zenith camera. The star image co-ordinates were estimated using the two main methods of centroid estimation, viz., *moment analysis and PSF fitting*. This paper compares these two methods of estimating image co-ordinates to sub-pixel level and their accuracies. Results so far indicate that star image measurement accuracies better than 0.3 arcsecond can be obtained. They also show that PSF fitting method is more adaptive to automation.

1. Introduction

Stars are point sources. However the image formed of stars by focussing through a lens is not a point but a blurred spot. Thus point sources emit light which is processed by the optical system, because of diffraction (and the possible presence of aberration) (Kovalevsky, 1995), this light is smeared out into some sort of blur spot over a finite area on the image plane rather than focus to a point (Jain, 1989). When this patch is scanned the distribution of intensities can be described by a mathematical function. This function is known as the point spread function (PSF) of the lens. It is the impulse response of the system whether it is optically perfect or not. In a well corrected system, apart from a multiplicative constant the PSF is the Airy irradiance distribution function (Longhurst, 1967) centred in the Gaussian image point. The value of the spread function depends only on the displacement of that location from the particular image point on which the PSF is centred (Bove, 1993; Horn, 1986).

For an object spread across an area or several pixels the object is no more just a point. We must therefore give a precise meaning to the term 'co-ordinates' or 'position'. In order to determine the co-ordinate of the object, the centre of area is chosen as the representative position. The centre of area is estimated by the centre of mass or centroid of the object. Also determining the position of a star by just taking

(clicking on) the position of its maximum intensity would at best give the precision of measurement to one pixel. It is therefore highly preferable to determine the centre of mass or centroid (Eissfeller and Hein, 1994; Buil, 1991).

The concept of estimation in image processing relates to the evaluation of image parameters, that is, considered to be relevant to the characterisation of the objects in the image. Thus our image analysis problem will involve measurements of certain characteristics of the image. These include;

- 1 intensity
- 2 geometric features
- 3 centroid.

1.1 Geometric Features

These include the following;

LENGTH: The length of a line (L) in a discrete image is the distance between the centres of the pixels.

$$L = d - 1 \quad (1)$$

where d is the number of pixels the line covers. If an object occupies one pixel, its length is zero.

PERIMETER: The perimeter (P) is equal to the sum of the side lengths.

$$P = \sum \text{side lengths} \quad (2)$$

AREA (A): This is equal to the sum of all the pixels covered by the object. That is, area of an object in a digital image is the number of points in the object. Thus we can compute the area of the object by simply scanning these points

$$A = \text{total number of pixels} \quad (3)$$

Measurement of perimeter or area are only meaningful provided area > perimeter (for calculations to be accurate). If object is larger than one pixel the better the area measurement. Thus for better centroid estimation the image should be spread over 2 or more pixels.

2. Principles of Centroiding

There are two basic techniques used to estimate the centroid of a star object. They are;

- 1 the image moment analysis
- 2 profile fitting or point spread function (PSF) fitting.

2.1 IMAGE MOMENTS

When a set of values has a tendency to cluster around some particular value, then it may be useful to characterize the set by a few numbers that are related to its *moments*, the sums of integer powers of the values (Horn 1986 pp.34, Press et al 1992 pp. 610-613). If an object in an image is defined by the function $B(x,y)$, then the moments generated by this function give interesting features of the object. For digital images the (k+l)th order is defined by Papoulis theorem (Gonzalez and Wintz 1987 pp. 421).

$$B_{KL} = \sum_x \sum_y x^K y^L B(x, y)$$

The total intensity of the image is given by B_{00} . We find that moments depend on the intensity or grey level. One important thing about moment features of objects is that they can be used regardless of location in the image and size of the object. Image moments include the following; centre of mass, variance and orientation.

CENTRE OF MASS: If we regard the intensity or grey level $B(x,y)$ at each point (x,y) of the given image (B) as the "mass" of (x,y), we can define the centroid (centre of mass) as well as the other moments of B. It is that point where all the mass of an object could be concentrated without changing the first moment of the object about any axis. The centre of mass is the centre of area of a figure which in practice is chosen as the position of the figure. In the two dimensional case, the center of mass is given by (B_{10}, B_{01}) .

$$B_{10} = \sum \sum x B(x, y) / B_{00}$$

$$B_{01} = \sum \sum y B(x, y) / B_{00}$$

VARIANCE (σ^2): This is given by the second moment about the centre of mass (B_{KL}^C)

$$\sigma_x^2 = B_{20}^C = B_{20} - B_{10}^2$$

$$\sigma_y^2 = B_{02}^C = B_{02} - B_{01}^2$$

σ_x^2 characterises the extension or spread of the object in the x direction.

ORIENTATION (θ): This is defined as the angle of axis of the least moment of inertia. It determines how the object lies in the field of view (Horn 1986 pp. 49). The orientation of an image is given by (ibid. pp. 54):

$$\tan(2\theta) = \frac{2B_{11}}{B_{20} - B_{02}}$$

unless $B_{11} = 0$ and $B_{20} = B_{02}$. Consequently

$$\sin(2\theta) = \frac{\pm 2B_{11}}{\sqrt{(2B_{11})^2 + (B_{20} - B_{02})^2}}$$

$$\cos(2\theta) = \frac{\pm (B_{20} - B_{02})}{\sqrt{(2B_{11})^2 + (B_{20} - B_{02})^2}}$$

For a circular object orientation is 0 as it is isotropic. From the above equations the position, variance and orientation of an object can be calculated using first and second moments only. These moments are invariant under linear co-ordinate transformations (Jain 1989 pp. 381). Thus we do not need the original image to obtain the first and second moments. Projections of the image are sufficient. This is of great interest since the projections are more compact and suggest faster algorithms (Horn 1986 pp.54). Existing literature gives the accuracy of the simple moment centroiding algorithm to be between 0.05 to 0.1 pixel (Schildknecht 1994, Chubunichev pp.152-153).

2.2 PSF Fitting

The basic principle in this technique is that all images of stars on a CCD frame have, barring distortion introduced by the camera optics, the same form but differ from one another in intensity or scaling ratio and position. (Teuber, 1993). Thus fitting a suitable defined PSF to a series of images will give relative magnitudes

$$m = z_{pt} - 2.5 \log(\text{scaling ratio}) \quad (9)$$

where z_{pt} is the magnitude assigned to the PSF. Mathematical curves are fitted to the real data until a good match is obtained. The parameters determined are the position and the scaling ratio. The mathematical equation used to model the profile of the stellar image is usually the Gaussian function (Buil, 1991).

$$I(r) = I(0) \exp\left(-\frac{r^2}{2\sigma^2}\right) \quad (10)$$

where:

r is the radius with respect to the centre of the star image

σ is a parameter characterizing the stars spreading

$I(0)$ is the maximum intensity

Linearizing equation (10) we get

$$\ln I(r) = \ln I(0) + br^2 \quad (11)$$

The equation above is of the form $Y = A + BX$. The coefficients (A,B) can be estimated by linear regression from (X,Y) pairs.

$$A = \frac{S_X S_{XY} - S_{XX} S_Y}{S_X^2 - n S_{XX}} \quad (12)$$

$$B = \frac{S_X S_Y - n S_{XY}}{S_X^2 - n S_{XX}}$$

and

$$S_X = \sum_{i=1}^n X_i ; S_{XX} = \sum_{i=1}^n X_i^2 ; S_Y = \sum_{i=1}^n Y_i ;$$

$$S_{XY} = \sum_{i=1}^n X_i Y_i .$$

Expressing r in terms of image co-ordinates gives

$$r_i^2 = (x_i - x_0)^2 + (y_i - y_0)^2 \quad (13)$$

Replacing r in equation (11) by equation (13) we get.

$$\ln I(r_i) - \ln I(0) = b \left[(x_i - x_0)^2 + (y_i - y_0)^2 \right] \quad (14)$$

The above equation can be written as

$$E_i = c_0 + c_1 x_i + c_2 y_i + c_3 x_i^2 + c_4 x_i^2 \quad (15)$$

where $E_i = \ln I(r_i) - \ln I(0)$, i is the pixel number and (x_i, y_i) are pixel co-ordinates;. The centroid, (x_0, y_0) , of the image is computed after solving for the coefficients, c_j ($j=0..4$) of equation (15) using the least squares criterion. Differentiating (15) and using the necessary conditions for extremum gives;

$$\frac{\partial E}{\partial x} = c_1 + 2c_3 x = 0$$

$$\frac{\partial E}{\partial y} = c_2 + 2c_4 y = 0 \quad (16)$$

putting $x = x_0$ and $y = y_0$ in (59) we get

$$x_0 = -\frac{c_1}{2c_3}$$

$$y_0 = -\frac{c_2}{2c_4} \quad (17)$$

It is obvious from equation (15) that the PSF fitting method, unlike moment analysis, can only be used when the star image is spread over more than four pixels. However the process can be easily extended to fitting many images simultaneously. This allows position determination in a much more crowded situation and complete automation of the whole process. It is said to give better accuracy than the moment analysis method (Schildknecht, 1994). Thus for accuracies better than 0.05 one has to use the PSF fitting method. Theoretical estimations by Eisfeller and Hein (Eisfeller and Hein, 1994) using the PSF fitting method gave accuracies of the order of 0.05 to 0.15 of a pixel.

3. ImageCo-ordinate Measurements

In this experiment centroids of real star objects were determined using both the moment analysis and PSF fitting methods and analyzed:

- A To find out the measuring accuracy of CCD co-ordinates of star images that can be achieved in practice.
- B To compare the two methods

In this work images were taken using the *IFEN* CCD integrated telescope with exposure times ranging from 1 to 3 seconds and the telescope pointing to the zenith. These exposure times were found to be optimum, in terms of avoiding trails and obtaining good signal-to-noise ratios, after many trials. All the sets of images were multiple images of four. The sequence of operations described below were followed throughout the observations;

- 1 Set up the instrument
- 2 Check instruction status from operator
- 3 Prepare the CCD - unrecorded readouts to flush
- 4 Open the shutter for a time period
- 5 Close the shutter
- 6 Readout the CCD according to a precise pattern
- 7 Digitize the signal from each pixel
- 8 Store the data in a computer
- 9 Return the CCD to a standby mode if appropriate.

Apart from 1 and 2 all the other events occurred in time sequence under computer control.

The images were calibrated based on equation (18) below (Buil, 1991) and then median filtered (Teuber, 1993; Raab, 1996), to smooth or minimize image noise, after which the centroid of star objects were measured.

$$I_c(x, y, t) = K \frac{I_o(x, y, t) - N(x, y, t)}{F(x, y, t') - N'(x, y, t')} \quad (18)$$

where

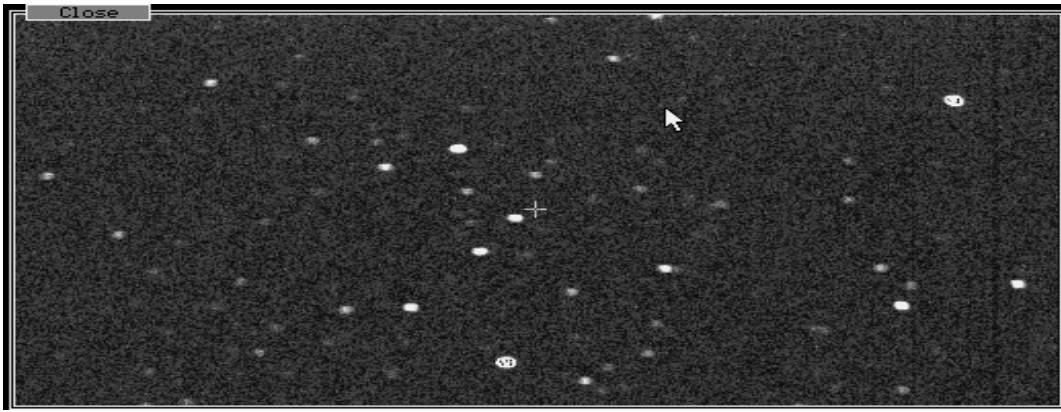


Figure 1: CCD250_2 a 2.5 sec. exposure image after calibration and median filtering

Two sets of observations were used. The centroids in the first set, found in table 4, were determined with the moment analysis software, *astrometrica*, developed by Raab (Raab, 1996) while the second set made up of 17 multiple images taking under 45 minutes found in table 5 were determined by both moment analysis and PSF fitting methods using *astrometrica* and the *CCD software* developed by Ploner (Ploner, 1996) respectively. The PSF fitting method was found to be more adaptive to geodetic use.

4. Analysis of Results

Before the analysis the image co-ordinates which were given in pixels were converted to sensor co-ordinate, also in pixels, using the following expressions.

$$x - \text{sensorco-ordinate} = \text{columnmeasured} - \frac{\text{total columns}}{2} \quad (19)$$

$$y - \text{sensorco-ordinate} = \frac{\text{total rows}}{2} - \text{row measured}$$

It is pertinent to note that the images were taken independently and secondly the stars were in motion. In order to analyse these images they were registered or transformed to the same datum using the two-dimensional similarity transformation. The transformation also gives

t is the integration time of the image to be reduced
 t' is integration time of the flat-field

$N(x, y, t)$ is the dark map of the image to be reduced

$N'(x, y, t)$ is the dark map of the flat-field

K is the multiplicative coefficient - It is equal to the the average intensity of the flat-field. It allows us to find, approximately, the initial level of the reduced image.

One of the images used for the analysis is shown in figure 1 below. The common images in every multiple image was identified and their co-ordinates measured.

mean positions (x_j^m, y_j^m) , of the common points in the new co-ordinate system. These serve as approximate co-ordinates in the least squares computations described below.

4.1 Computations

Our basic mathematical model, equation (17), is of the form

$$\begin{pmatrix} x_j \\ y_j \end{pmatrix} = \begin{pmatrix} a_i & b_i \\ -b_i & a_i \end{pmatrix} \begin{pmatrix} x_{ij}' \\ y_{ij}' \end{pmatrix} + \begin{pmatrix} e_i \\ f_i \end{pmatrix} \quad (20)$$

Similarly we have

$$\begin{pmatrix} x_j^m \\ y_j^m \end{pmatrix} = \begin{pmatrix} a_i & b_i \\ -b_i & a_i \end{pmatrix} \begin{pmatrix} x_{ij}^c \\ y_{ij}^c \end{pmatrix} + \begin{pmatrix} e_i \\ f_i \end{pmatrix} \quad (21)$$

or

$$\begin{pmatrix} x_{ij}^c \\ y_{ij}^c \end{pmatrix} = \begin{pmatrix} a_i & -b_i \\ b_i & a_i \end{pmatrix} \begin{pmatrix} x_j^m - e_i \\ y_j^m - f_i \end{pmatrix} \quad (22)$$

since $\begin{pmatrix} a & b \\ -b & a \end{pmatrix}$ is orthogonal. (x_{ij}^c, y_{ij}^c) are computed image co-ordinates.

$$\text{Let } \begin{pmatrix} x_j \\ y_j \end{pmatrix} = \begin{pmatrix} x_j^m + dx \\ x_j^m + dy \end{pmatrix} \quad (23)$$

Substituting equation (23) into (20) combining with (21) and rearranging we get the observation equation

$$\begin{pmatrix} x_{ij}' - x_{ij}^c \\ y_{ij}' - y_{ij}^c \end{pmatrix} = \begin{pmatrix} a_i & -b_i \\ b_i & a_i \end{pmatrix} \begin{pmatrix} dx_j \\ dy_j \end{pmatrix} \quad (24)$$

This is of the form

$$L - L_c = AdX \quad (25)$$

As there were more observations than unknowns, the system of equations produced an overdetermined problem. The least squares criterion was applied by introducing residuals or improvements \mathbf{v} to the observations or measured co-ordinates \mathbf{L}

$$\mathbf{v} = AdX - (L - L_c) = AdX - \mathbf{b} \quad (26)$$

where

- \mathbf{v} is vector of residuals
- $d\mathbf{X}$ is vector of corrections or unknowns
- \mathbf{A} is the design matrix
- \mathbf{L}, \mathbf{L}_c are measured and computed image co-ordinates
- \mathbf{b} is the vector of reduced measurements ("observed - computed")

From the observation equations normal equations were formed with weights (\mathbf{W}) obtained from the differences

between the transformed image co-ordinates and their mean co-ordinates in the common datum.

$$\mathbf{A}^T \mathbf{W} \mathbf{A} d\mathbf{X} = \mathbf{A}^T \mathbf{W} \mathbf{b} \quad (27)$$

It is pertinent to note that the adjusted quantities are rather insensitive with respect to the chosen weights but the estimates of their accuracies depend on them.

After the solution of the normal equations, using Cholesky's method, the residuals were computed from equation (26). From the residuals, the unit variance (σ_0^2) was computed from the formula:

$$\sigma_0^2 = \frac{\mathbf{v}^T \mathbf{W} \mathbf{v}}{n - u} \quad (28)$$

where n is the number of observation equations u is the number of unknowns. σ_0 is t-distributed with degree of freedom $(n-u)$ (Cross, 1990). It was used to test our model assumptions. If the number of common points is p , and the number of images m then $n = 2 \cdot p \cdot m$ and $u = 2 \cdot p$. The covariance matrix (\mathbf{C}_{xx}) of the unknowns were given by:

$$\mathbf{C}_{xx} = \sigma_0^2 \mathbf{Q}_{xx} \quad (29)$$

here $\mathbf{Q}_{xx} = (\mathbf{A}^T \mathbf{W} \mathbf{A})^{-1}$. The standard errors of the estimated image co-ordinates were obtained by taking the square roots of the diagonal elements of \mathbf{C}_{xx} . An output of the computer program developed for the computations is shown in tables 1 to 3. The mean of the standard errors for every multiple image were calculated.

Table 1: Registration of images from a multiple exposure (CCD250)

transformation coefficients				
parameters	CCD250_1	CCD250_2	CCD250_3	CCD250_4
a	0.999989	1.000764	1.001095	1.001147
b	0.000000	0.000650	0.001269	0.001253
e	0.0024	63.1416	125.7476	186.3867
f	0.0008	1.2146	2.1138	3.0443

Table 2: mean co-ordinates of common points obtained from registration of CCD250

N ö.	approximate co-ordinates	
	x	y
1	-89.508504	161.702235
2	775.377367	-250.067488
3	-46.603056	-107.226853
4	-181.709226	-254.362887
5	1000.754835	-193.576459
6	22.083467	-19.701759
7	314.430090	-152.744945
8	-231.295036	113.951123
9	-571.988830	335.302454
10	158.202097	-447.477262
11	213.473261	397.919030
12	-308.908831	-259.834326
13	734.470882	-151.290134

Table 3: LSEs of image co-ordinates and their standard errors in pixels

UNIT VARIANCE = 0.9888 SQRT(UNIT VARIANCE) = 0.9944				
No.	x	y	std. error in x	std. error in y
1	-89.22597	161.613851	0.078854	0.100746
2	774.74013	-249.974204	0.1444	0.058467
3	-46.555306	-107.169811	0.134966	0.070193
4	-181.13891	-254.122311	0.104106	0.078838
5	1000.11368	-193.24504	0.597228	0.078465
6	22.129985	-19.744222	0.080516	0.120452
7	314.376728	-152.72932	0.262623	0.111357
8	-230.54873	113.894483	0.082132	0.074879
9	-571.305709	334.916241	0.168539	0.237849
10	158.198397	-446.811075	0.149174	0.057951
11	213.432419	397.561949	0.25563	0.46745
12	-308.468783	-259.49293	0.171369	0.231906
13	733.728221	-151.29214	0.572654	0.080937
mean std. error in x: 0.215553 mean std. error in y: 0.136114				

The results of the experiment are shown in table 4 and 5.

Table 4: Precision of centroid determinations from moment analysis method

image name	Date	Exp.time in secs.	No. of common objects	Unit variance σ_o^2	mean standard errors (in pixels)	
					σ_x	σ_y
CCDF100	11.11.96	2	8	1.03	0.18	0.13
CCDF201	10.02.97	1	12	1.08	0.32	0.29
CCDF212	23.02.97	2	12	1.04	0.12	0.10
CCDF302	23.02.97	2	12	1.04	0.16	0.13
CCDF303	23.02.97	2	10	1.02	0.19	0.10
CCDF116*	23.02.97	1.6	8	1.05	0.44	0.43
CCDF224*	23.02.97	2.4	8	2.94	0.89	0.84
CCDF225	23.02.97	2.5	8	1.02	0.35	0.34
CCDF228	23.02.97	2.8	8	1.04	0.37	0.33

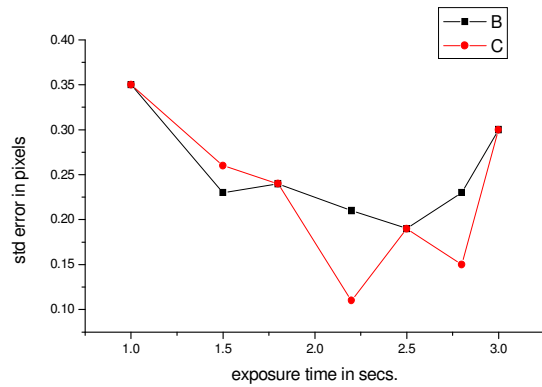


Figure 2A: Relation between image co-ordinate accuracies and exposure time from PSF fitting

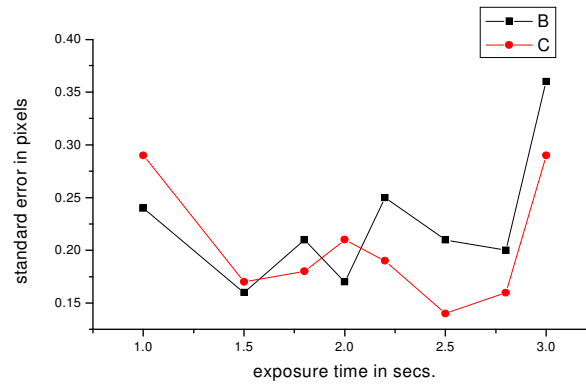


Figure 2B: Relation between image co-ordinate accuracies and exposure time from moment analysis

Table 5: Precision of centroid determinations from moment analysis and PSF fitting metho

Serial No.	Image name	Time of observation (UTC)	Exp. time (secs)	Moment analysis (in Pixels)			Psf fitting (in Pixels)		
				σ_o^2	σ_x	σ_y	σ_o^2	σ_x	σ_y
1	CCD101*	21:45:59	1	0.99	0.47	0.46	1.03	0.32	0.39
2	CCD120*	21:47:59	1.2	1.23	0.56	0.53	1.09	0.40	0.37
3	CCD150	21:57:59	1.5	1.03	0.27	0.29	1.10	0.09	0.15
4	CCD180*	21:59:54	1.8	1.04	0.37	0.40	1.04	0.34	0.24
5	CCD181	22:01:19	1.8	1.01	0.24	0.24	1.01	0.21	0.18
6	CCD200*	22:02:32	2	1.27	0.61	0.60	1.04	0.43	0.42
7	CCD201*	22:03:59	2	1.48	0.45	0.43	1.09	0.17	0.21
8	CCD220	22:09:51	2.2	0.98	0.21	0.11	1.05	0.25	0.19
9	CCD221	22:10:58	2.2	0.99	0.23	0.23	-	-	-
10	CCD250	22:13:34	2.5	1.10	0.19	0.23	1.02	0.22	0.14
11	CCD251	22:12:11	2.5	1.05	0.14	0.14	1.05	0.14	0.11
12	CCD280	22:13:11	2.8	1.05	0.17	0.10	-	-	-
13	CCD281	22:16:19	2.8	1.04	0.23	0.15	1.01	0.20	0.16
14	CCD301	22:18:33	3	1.02	0.18	0.13	1.04	0.36	0.29
15	CCD253	22:19:58	2.5	1.09	0.23	0.19	1.03	0.26	0.18
16	CCD103	22:24:06	1	0.99	0.23	0.23	1.03	0.16	0.10
17	CCD153	22:28:17	1.5	1.03	0.18	0.22	0.99	0.22	0.18

This corresponds to an accuracy better than 0.3 arcsecond for imaging systems of focal length greater than or equal to 80 cm. and pixel size of 10 μ m. The effect of the apparent cloudy weather on the standard errors shown in table 4 and 5 and the erratic behaviour of the graphs above indicates that one of the main limiting factors of the centroid determination of star objects is the prevailing weather condition rather than the method used. However it appears that the moment analysis method is more prone to bad weather.

5. Conclusion

The above experiment, analysis and results show that an accuracy of 0.1 pixel can be achieved and that there is no significant difference in the accuracy that can be achieved between the two main methods of centroid estimation, viz, *moment analysis and PSF fitting*. It also confirms the theoretical findings mentioned in section [2.2]. This indicates that it is possible to obtain image measurement accuracies better than the ± 0.3 arcsecond required for astro-geodetic determinations using portable telescopes, i.e., focal lengths between 80 and 150 cms. The analysis also showed that centroid estimates deteriorate with bad or cloudy weather more seriously in the case of moment

analysis. Furthermore during the centroid measurements it was found that the PSF fitting method is more adaptive to automation.

References

1. **Bove, V.M. Jr.** (1993); Entropy based depth of focus. Journal of Optical Society of America Vol. 10 No. 10
2. **Buil, C.** (1991); CCD Astronomy : CCD Astronomy, construction and use of an Astronomical CCD Camera. William-Bell Inc. Virginia.
3. **Chubunichiev, A.**; Algorithms of digital target location and their investigations. ISPRS Journal Vol. XXIX Commission V
4. **Cross, P.A.** (1990); Advanced least squares applied to position fixing (working papers). North East London Polytechnic.
5. **Eisfeller B., G.W.Hein;** (1994); Astrogeodetic levelling with an Integrated DGPS/CCD star

- camera system. Proceedings of the International Symposium on Navigation (KISS 94) Calgary Canada.
6. **Horn, B. K. P.** (1986); Robot vision. The MIT Press, Massachusetts.
 7. **Gonzalez, R.C., P. Wintz** (1987); Digital image processing. Addison Wesley Publishing Co.
 8. **Jain, A. K.** (1989); Fundamentals of image processing. Prentice Hall Inc., New Jersey
 9. **Kovalevsky, J.** (1995); Modern Astronomy. Springer Verlag, Berlin Heidelberg
 10. **Longhurst, R. S.** (1967); Geometrical and Physical Optics. Longmans, London.
 11. **Press, W. H., W.T. Vetterling, S.A. Teukolsky, B.P. Flannery** (1995); Numerical recipes in C. Cambridge University Press.
 12. **Ploner, Martin** (1996); CCD-Astronomie von objekten des geostatiären ringes. Geowissenschaftliche Mitteilungen Heft 46. Technical University Vienna.
 13. **Raab, H.** (1996); Astrometrica software version 3.1
 14. **Schildknecht, T.** (1994); Optical astronomy of fast moving objects using CCD detectors. Swiss Geodetic Commission.
 15. **Teuber, J.** (1993); Digital image processing . Prentice Hall International (UK)